



## OPEN ACCESS

## EDITED BY

Yang Yang,  
Yangzhou University, China

## REVIEWED BY

Wang Hongliang,  
Changzhou Institute of Technology,  
China

Weixuan Jiao,  
Yangzhou University, China  
Leilei Ji,  
Jiangsu University, China

## \*CORRESPONDENCE

Tianliang Lin,  
✉ ltlkxl@163.com

RECEIVED 16 March 2023

ACCEPTED 01 June 2023

PUBLISHED 19 June 2023

## CITATION

Xu X, Lin T, Ren H, Guo T, Li Z and Miao C (2023), Research on electro-hydraulic composite drive winch and energy recovery system for mobile crane. *Front. Energy Res.* 11:1187558. doi: 10.3389/fenrg.2023.1187558

## COPYRIGHT

© 2023 Xu, Lin, Ren, Guo, Li and Miao. This is an open-access article distributed under the terms of the [Creative Commons Attribution License \(CC BY\)](https://creativecommons.org/licenses/by/4.0/). The use, distribution or reproduction in other forums is permitted, provided the original author(s) and the copyright owner(s) are credited and that the original publication in this journal is cited, in accordance with accepted academic practice. No use, distribution or reproduction is permitted which does not comply with these terms.

# Research on electro-hydraulic composite drive winch and energy recovery system for mobile crane

Xianggen Xu<sup>1,2</sup>, Tianliang Lin<sup>1,2\*</sup>, Haoling Ren<sup>1,2</sup>, Tong Guo<sup>1,2</sup>, Zhongshen Li<sup>1,2</sup> and Cheng Miao<sup>1,2</sup>

<sup>1</sup>College of Mechanical Engineering and Automation, Huaqiao University, Xiamen, China, <sup>2</sup>Fujian Key Laboratory of Green Intelligent Drive and Transmission for Mobile Machinery, Xiamen, China

Owing to the high power consumption and limited control precision of traditional hydraulic drive winch systems, this study proposes hydraulic and electric-type energy recovery systems. The accumulator used in the hydraulic type has low energy density, which makes it difficult to store a large amount of energy. Meanwhile, the electric motor/generator used in the electric type cannot solve the secondary slip because of oil leakage, which leads to low controllability and high-power consumption under near-zero speed and high torque conditions. Thus, based on electric construction machinery with high-pressure, energy-dense electric energy storage units, this study proposes an electro-hydraulic composite drive winch and energy recovery system and control strategy for mobile cranes. Considering the good control characteristics of the electric motor/generator and the high-power density of the hydraulic accumulator, this hydroelectric composite drive and energy recovery system may solve the secondary sliding challenge and ensure large torque output at near-zero speed. A simulation model of the mobile crane is established to verify the feasibility of the proposed system and control strategy. The research results showed that the system is more efficient at recovering energy when the weight is lowered by a greater distance.

## KEYWORDS

winch system, engineering machinery, secondary slip, mobile crane, electro-hydraulic composite drive, energy recovery efficiency

## 1 Introduction

With global warming, rising oil prices, and the energy crisis, the importance of energy saving and emission reduction has been gradually increasing in numerous guiding frameworks (Zhang et al., 2017; Liu, 2019). Construction machinery often has a large amount of negative load during movement. Reducing carbon emissions and implementing electrification to achieve energy saving and environmental protection are of current interest worldwide (Lin et al., 2020). The types of winch energy-saving drives are divided according to their components into hydraulic drive, electro-hydraulic composite drive, and direct electric motor/generator drive. Similarly, according to the energy storage components, winch energy recovery can be divided into hydraulic recovery, electric recovery, and composite recovery.

The winch systems of traditional construction machinery are primarily hydraulic drives. Central South University proposed an energy-saving system for the recovery of the potential energy of the main lowering winch of rotating drilling rigs, in which the secondary element

hydraulic pump/motor was mechanically connected to the engine in a coaxial manner, and the accumulator recovered the residual potential energy (Zhu et al., 2018). Fang at Central South University designed a hybrid oil-electric winch system based on the hydraulic system for the main winch of rotary drilling rigs, in which the hydraulic motor/generator was used to recover the potential energy into electric energy stored in the supercapacitor when the main winch was lowered (Fang et al., 2012). Bolonne, at the University of Molétouvo, proposed a hybrid system for RTG cranes that included a lithium battery, a supercapacitor, and a diesel generator, in which the supercapacitor and lithium battery worked together to recover the crane's regenerable energy (Bolonne and Chandima, 2019). Kim at the Korean Classification Society proposed a hybrid system using diesel generators in combination with supercapacitors and lithium-ion batteries and assessed energy recovery into lithium batteries and supercapacitors under different operating conditions. The results showed that the system could significantly reduce harmful emissions (Kim et al., 2019). Corral-Vega of the University of Cadiz proposed an RTG drive scheme using a fuel cell as the energy source and a supercapacitor as the energy storage system. The simulation results demonstrated the high energy efficiency of the hybrid system. Direct-drive winches are primarily used in stationary machinery, such as tower cranes, shovels, and elevators. Huang from Beijing Jiaotong University proposed a supercapacitor-based power compensation and energy recovery system for mine hoisting equipment, in which the energy of the shaft grid and the potential energy of the shaft repair machine were stored in the supercapacitor through a converter (Huang Pu, 2015). The results showed that the system was more practical at obtaining power and the load was lower. Li from ZOOMLION researched a purely electric truck crane energy recovery device and system strategy in unplugged and plugged operation conditions, and verified the effectiveness of the crane winch energy recovery device and control strategy (Li et al., 2022). Research on electric winches has focused on electrical control devices (Premkumar and Manikandan, 2014; Kodkin and Anikin, 2020). A control device was used to prevent backlash due to slack in the traction component (Lee et al., 2019; Caporali, 2021). In addition, there are control algorithms that compensate for the loss of torque in the low-speed area of the motors (Li and Wang, 2019; Roman et al., 2021), and mechanical methods to improve the structure and stability to provide ordered coiling of strings, etc. Electro-hydraulic composite drive winch systems have used electric motor-hydraulic pumps/motors to supplement the composite drive and the power regeneration system. Liu of the Taiyuan University of Technology proposed an electro-hydraulic hybrid drive winch potential energy recovery system, which used an electric motor as the main drive to reduce throttling losses, combined with a hydraulic pump/motor and accumulator as the energy recovery unit. The results showed that the electro-hydraulic composite drive winch system had good energy recovery (Liu et al., 2022). Zhao of the Taiyuan University of Technology applied the composite electric motor-hydraulic pump/motor composite drive system to an elevator system, which recovered energy from the traction machine's power generation state through the accumulator, and released the energy from the accumulator when the traction machine needed to be in the electric state for energy recovery (Zhao et al., 2016; Zhang et al., 2020). Wang Xthe at the Taiyuan University of Technology proposed a hybrid electro-hydraulic drive electric excavator hoist system, which utilized the engine as the main drive and the accumulator-hydraulic pump/motor as the auxiliary

drive. The potential energy of the hoist system was mainly stored in the accumulator through the hydraulic pump/motor when the hoist system was lowered. The energy was released by the accumulator when it was lifted (Wang et al., 2020). The hydraulic pump/motor and the electric motor worked together to complete the lifting. The simulation results showed that the system reduced the power consumption by approximately 30% compared to the traditional system. Zhang of the Dalian University of Technology proposed a composite electro-hydraulic drive hoist system, in which the speed was controlled by a hydraulic system and the torque was controlled by an electric motor. The hydraulic motor was connected to the two ends of the bobbin to drag the load together. The results showed that the system energy recovery efficiency was approximately 60% (Zhang, 2019).

To recover the potential energy of the mobile crane winch system and reduce engine pollution, considering the good control characteristics of the electric motor/generator and the high power density of the hydraulic accumulator, this study proposes a hydro-electric composite drive and energy recovery system to solve the challenge of secondary sliding and ensure the large torque output at near-zero speed. A control strategy is also proposed to integrate energy recovery and regeneration for the proposed composite winch system.

## 2 Working principles of the winch system

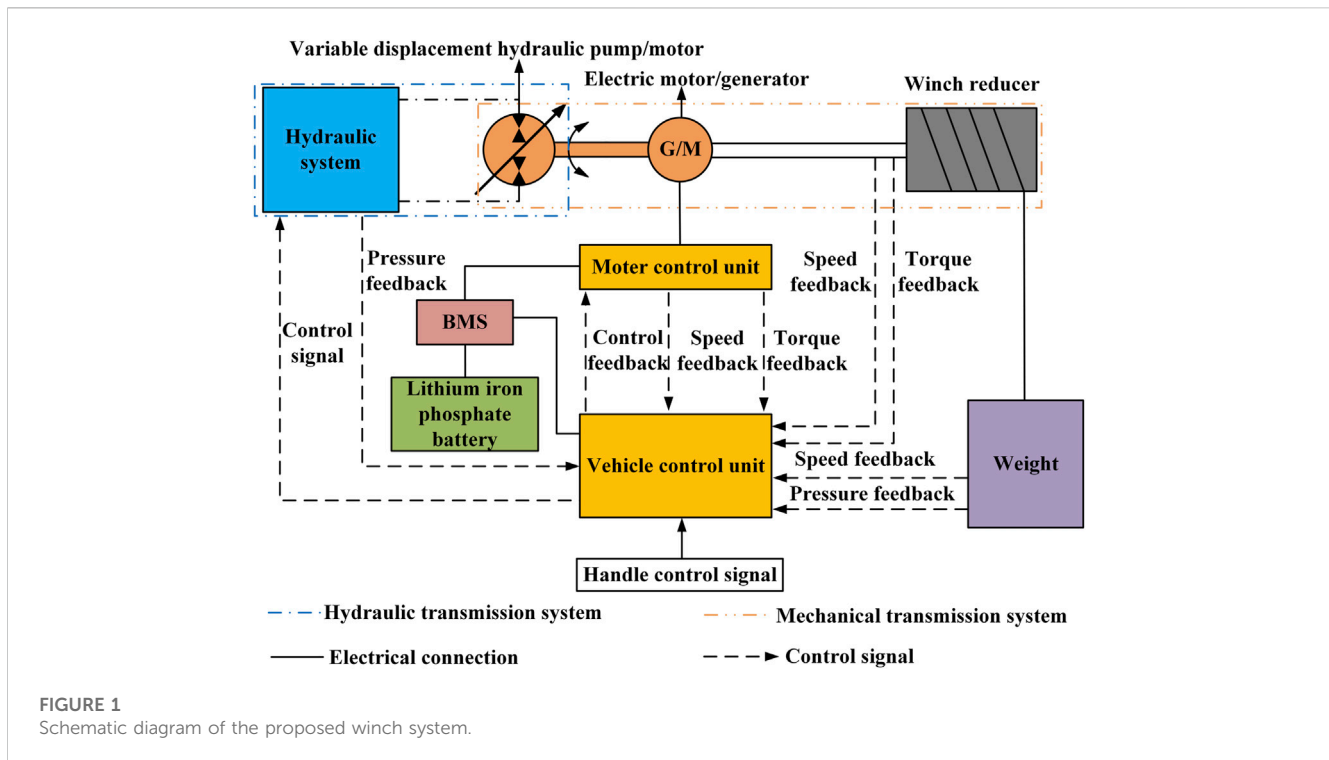
The scheme of the proposed entity electro-hydraulic composite drive winch system is shown in Figure 1. The system mainly contains an electrical component, a hydraulic drive component, and a mechanical drive component.

### 2.1 Electric drive component

The pressure signal from the hydraulic system, the speed and torque signal from the motor controller, and the artificially desired weightlifting speed signal are collected by the vehicle control unit (VCU). The control unit in the hydraulic system, the electric motor controller unit (MCU), and the lithium battery management system (BMS) receive the control signals from the VCU via the controller area network (CAN) bus and input and output (IO) port. The closed-loop enables cooperative control in multiple quadrants of the electric motor/generator-variable displacement hydraulic pump/motor output speed, angle, torque, and other parameters. The weight is driven to lift and lower to achieve the desired movement.

### 2.2 Hydraulic drive component

The hydraulic drive component is shown in Figure 2. In addition to storing energy, the high-pressure and low-pressure accumulators provide hydraulic energy to the variable displacement hydraulic pump/motor. Each 2-position, 2-way electromagnetic valve receives control signals from the VCU depending on the different working conditions. Hydraulic oil in both the high-pressure and low-pressure accumulators is transferred to the variable displacement hydraulic pump/motor. The oil is pressurized or depressurized and then returned to the high-pressure and low-pressure



accumulators via the 2-position, 2-way electromagnetic valve to complete the energy recovery. The differential pressure between the two ends of the variable-displacement hydraulic pump/motor changes continuously with changes in the pressure of the high-pressure and low-pressure accumulators. The variable-displacement hydraulic pump/motor receives control signals from the VCU to change the displacement to meet the required output torque, while the high-pressure and low-pressure accumulators satisfy the pressure conditions.

### 2.3 Mechanical drive component

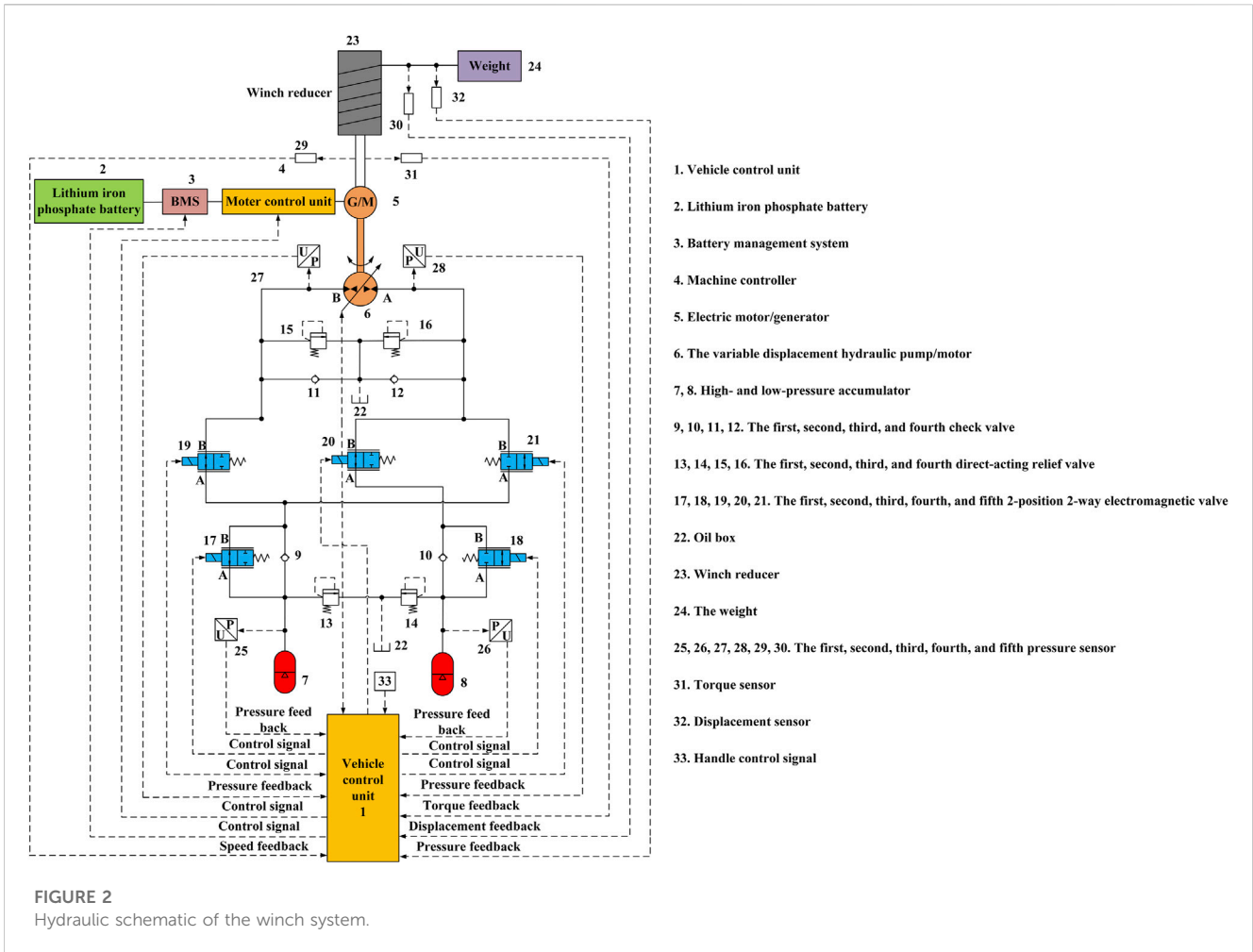
The mechanical drive component consists of coaxial mechanical coupling among the variable-displacement hydraulic pump/motor, electric motor/generator, and winch reducer. The weight is wound onto the winch reducer using a wire string. The winch reducer is driven by the electric motor/generator-variable-displacement hydraulic pump/motor controlled by the VCU. The weightlifting and lowering motion is determined by the VCU.

## 3 Control strategy and implementation process of the winch system

### 3.1 Analysis of the winch system control strategy

The signals of the pressure, displacement, torque, and SOC are input to the VCU through various sensors. The weightlifting and lowering motion mode differs depending on the load weight, the pressure difference between the high-pressure and low-pressure

accumulators, the low-pressure accumulator pressure, and the SOC. During the movement of the weight, the speed of the electric motor/generator is directly controlled by the handle opening. The displacement of the variable-displacement hydraulic pump/motor adapts itself to the speed. When a constant torque output of the variable-displacement hydraulic pump/motor is required, the VCU sends a corresponding control signal to each 2-position, 2-way electromagnetic valve and variable-displacement hydraulic pump/motor. The flow direction of the oil circuit and the displacement of the displacement hydraulic pump/motor change to achieve a constant torque output of the variable-displacement hydraulic pump/motor. The electric motor/generator for adaptive torque compensation and control strategy are shown in Figure 3, where  $Y_p$  is the handle opening (divided into positive and negative sides);  $Y_{min}$  is the positive and negative minimum handle opening;  $Y_{max}$  is the positive and negative maximum handle opening; SOC is the state of charge of the lithium battery;  $S_{max}$  is the maximum SOC value when potential energy recovery is performed;  $F$  is the negative load weight;  $F_{min}$  is the negative load weight when switching from purely electric motor/generator drive to electro-hydraulic composite drive;  $D_{17}$ ,  $D_{18}$ ,  $D_{19}$ ,  $D_{20}$ , and  $D_{21}$  correspond to the first, second, third, fourth, and fifth 2-position, 2-way electromagnetic valve, respectively;  $\Delta p$  and  $\Delta p_{min}$  are the differential pressure and minimum differential pressure between the high-pressure and low-pressure accumulators, respectively;  $p_1$  is the high-pressure accumulator pressure;  $p_2$  is the low-pressure accumulator pressure;  $p_{2min}$  is the minimum threshold pressure of the low-pressure accumulator; and  $p_{BA}$  is the differential pressure between B-port pressure  $p_B$  and A-port pressure  $p_A$  of the variable-displacement hydraulic pump/motor, i.e., the differential pressure between the two ends of the variable displacement hydraulic pump/motor.



- 1. Vehicle control unit
- 2. Lithium iron phosphate battery
- 3. Battery management system
- 4. Machine controller
- 5. Electric motor/generator
- 6. The variable displacement hydraulic pump/motor
- 7, 8. High- and low-pressure accumulator
- 9, 10, 11, 12. The first, second, third, and fourth check valve
- 13, 14, 15, 16. The first, second, third, and fourth direct-acting relief valve
- 17, 18, 19, 20, 21. The first, second, third, fourth, and fifth 2-position 2-way electromagnetic valve
- 22. Oil box
- 23. Winch reducer
- 24. The weight
- 25, 26, 27, 28, 29, 30. The first, second, third, fourth, and fifth pressure sensor
- 31. Torque sensor
- 32. Displacement sensor
- 33. Handle control signal

According to the aforementioned, the control strategy is as follows:

- (1) If the load weight satisfies  $F < F_{min}$  or the battery satisfies  $SOC \geq S_{max}$ , the handle opening satisfies  $Y_{min} < |Y_p| < Y_{max}$ ; the system is in the pure electric motor/generator drive and energy recovery mode. The electric motor/generator is in an electric motor state when the weight is lifting and in the electric generator state when it is lowering.
- (2) If the load weight satisfies  $F \geq F_{min}$  and the battery satisfies  $SOC < S_{max}$ , the handle opening satisfies  $Y_{min} < Y_p < Y_{max}$  and the differential pressure between the high-pressure and low-pressure accumulators satisfies  $\Delta p \geq \Delta p_{min}$ ; the system is in the electro-hydraulic composite drive mode. The electric motor/generator is working as the electrical motor. The variable-displacement hydraulic pump/motor is in a hydraulic motor state to allow the electro-hydraulic composite drive to lift the weight.
- (3) If the load weight satisfies  $F \geq F_{min}$  and the battery satisfies  $SOC < S_{max}$ , the handle opening satisfies  $-Y_{max} < Y_p < -Y_{min}$  and the low-pressure accumulator pressure satisfies  $p_2 \geq p_{2min}$ ; the system is in the recovery mode of the electro-hydraulic composite drive. The electric motor/generator is in the electric generator state. The variable-displacement hydraulic pump/

motor is in the hydraulic pump state to allow the electro-hydraulic composite drive to lower the weight.

### 3.2 Implementation process for the winch system

If the load is light ( $F < F_{min}$  or  $SOC \geq S_{max}$ ), the winch drive system operates in a purely electric motor/generator drive mode with an energy recovery mode and the electric motor/generator in an electric motor or power production state.

If the load is heavy ( $F \geq F_{min}$  and  $SOC < S_{max}$ ), the winch drive system initially operates in electro-hydraulic composite drive mode, in which the electric motor/generator is in the electric motor state and the variable-displacement hydraulic pump/motor is in the hydraulic motor state.  $D_{17}$ ,  $D_{19}$ , and  $D_{20}$  are energized and in a fully open state.  $D_{18}$  and  $D_{21}$  are de-energized. The hydraulic oil in the high-pressure accumulator reaches port B of the variable-displacement hydraulic pump/motor through  $D_{17}$  and  $D_{19}$ . The variable-displacement hydraulic pump/motor is then in the hydraulic-motor state. After depressurization, the oil is returned to the low-pressure accumulator from  $D_{20}$  and the second check valve. The pressures in both the high-pressure accumulator and the low-pressure accumulator, as well as the pressure at both ends of the

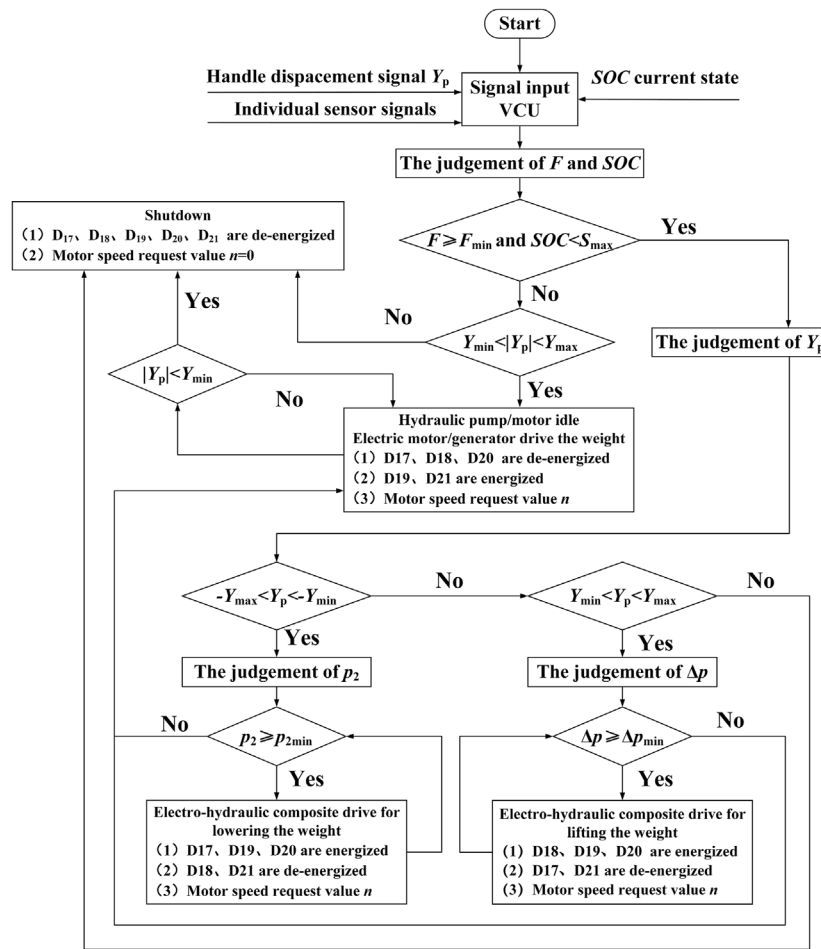


FIGURE 3 Control strategy for the winch system.

variable displacement hydraulic pump/motor, change with the above process. The displacement of the variable-displacement hydraulic pump/motor must be controlled to ensure that its output torque is constant and, thus, outputs a certain amount of power, as well as to control the motor controller to power the lithium battery to drive the electric motor/generator synergy to output the remaining power. If the differential pressure between the high-pressure and low-pressure accumulators cannot meet the constant torque output of the variable displacement hydraulic pump/motor; namely,  $\Delta p < \Delta p_{min}$  during the weight lifting,  $D_{17}$ ,  $D_{18}$ , and  $D_{20}$  are de-energized and  $D_{19}$  and  $D_{21}$  are energized and in a fully open state. The electric motor/generator alone outputs power to drive the winch reduction gear to lift the weight and drive the variable-displacement hydraulic pump/motor in the idle state. The first and second check valves and all four direct-acting relief valves work as required. In the work process described earlier, the speed of the electric motor/generator is directly controlled by the handle opening to achieve the target velocity of the weightlifting and complete the lifting motion.

If the load is heavy ( $F \geq F_{min}$  and  $SOC < S_{max}$ ), the winch drive system initially operates in the electro-hydraulic composite drive mode. The electric motor/generator is in the electric generator state and the variable displacement hydraulic pump/motor is in the

hydraulic pump state.  $D_{18}$ ,  $D_{19}$ , and  $D_{20}$  are energized and in a fully open state.  $D_{17}$  and  $D_{21}$  are de-energized. The hydraulic oil in the low-pressure accumulator reaches port A of the variable displacement hydraulic pump/motor through  $D_{18}$  and  $D_{19}$ . After pressurization, the oil is returned to the high-pressure accumulator from  $D_{20}$  and the first check valve. The pressures in both the high-pressure and low-pressure accumulators, as well as the pressure at both ends of the variable displacement hydraulic pump/motor, change during the above process. The displacement of the variable-displacement hydraulic pump/motor is controlled by the VCU to ensure a constant power output of the variable-displacement hydraulic pump/motor. The lithium is treated as a power source to ensure the remaining power output of the electric motor/generator. If the fluid pressure in the low-pressure accumulator is insufficient to keep the reverse towing torque formed by the variable-displacement hydraulic pump/motor at a certain value during the weight lowering; namely,  $p_2 < p_{2min}$ ,  $D_{17}$ ,  $D_{18}$ , and  $D_{20}$  will be de-energized.  $D_{19}$  and  $D_{21}$  will be energized and in a fully open state. The motor/generator alone outputs power to drive the winch reduction gear to lower the weight and make the variable-displacement hydraulic pump/motor in the idle state, and the first check valve, the second check valve, and all four direct-



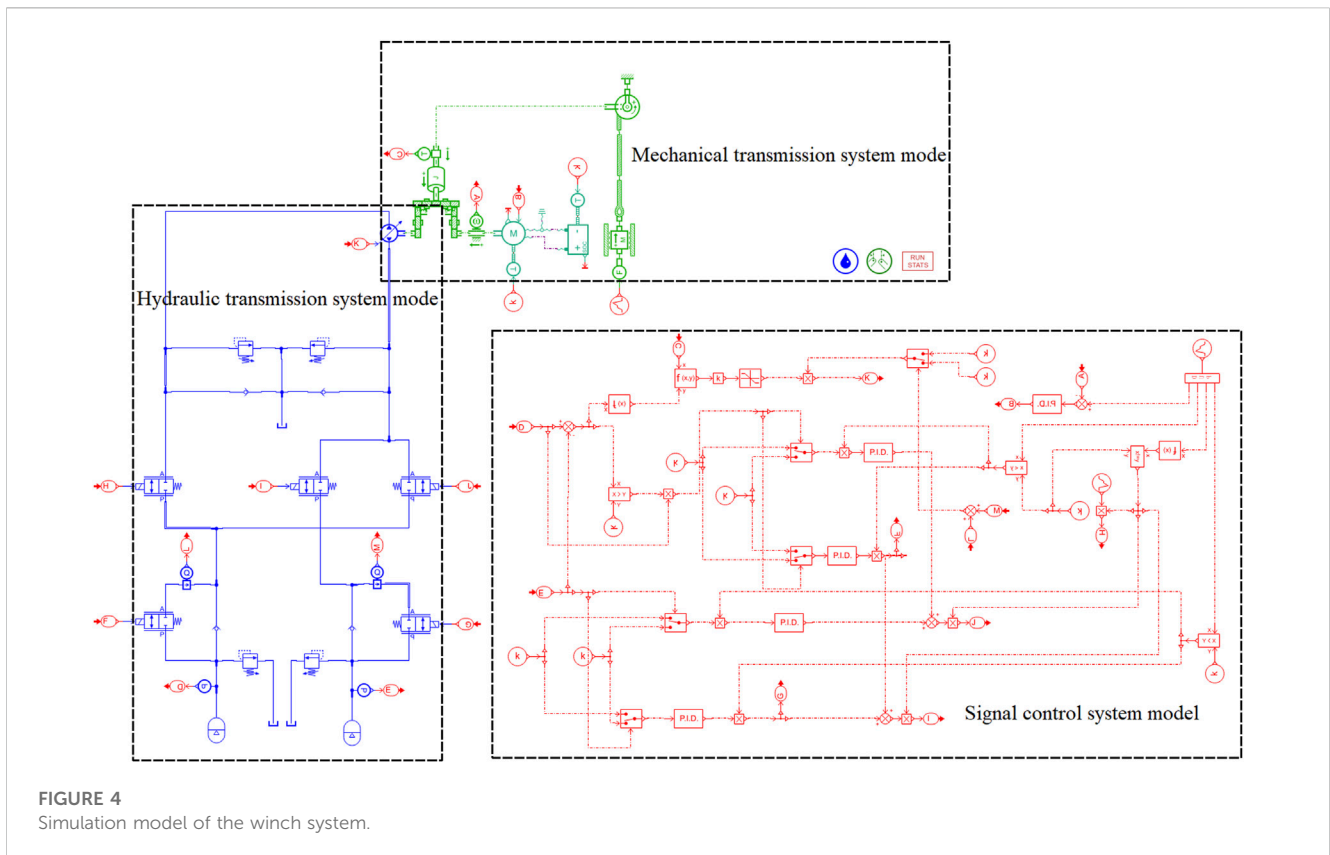


**FIGURE 4**  
Simulation model of the winch system.

**TABLE 1** Main simulation parameters of the winch system.

Parameter	Parameter value
Rated power of the motor	50 kW
Rated speed of the motor	3,600 r/min
Rated torque of the motor	130 N·m
Battery capacity	6.5 Ah
Initial battery charge	90% SOC
Winch gear ratio	55.2
Diameter of the winch reducer reel	0.44
Maximum velocity of the weight movement	1 m/s
Load weight range	1–4 t
Maximum displacement of the variable displacement hydraulic pump/motor	500 mL/r
Rated speed of the variable displacement hydraulic pump/motor	3,600 r/min
Opening pressure of the first direct-acting relief valve	20 MPa
Opening pressure of the second direct-acting relief valve	5 MPa
Opening pressure of the third direct-acting relief valve	20 MPa
Opening pressure of the fourth direct-acting relief valve	20 MPa

acting relief valves work as required. In the working process described above, the speed of the electric motor/generator is directly controlled by the handle opening to achieve the target lowering velocity of the weight.

When the winch must be stopped during the weight-lowering process, the handle opening should be reduced to below the minimum threshold. All the 2-position, 2-way electromagnetic valves are controlled in the de-energized state. The electric motor/generator is

controlled by the VCU in the blocked condition to stop the movement of the weight. The first check valve, the second check valve, and all four direct-acting relief valves work as required.

The system makes full use of the high energy density of the electrical energy storage unit and the good control characteristics of the electric motor/generator. The system also provides a solution to the problem of secondary sliding of heavy loads as well as the low energy density of the accumulator. The proposed closed hydraulic system using the accumulator-variable displacement hydraulic pump/motor can achieve high power density and high torque output at near-zero speed and solve the problem of high energy consumption of the electric motor/generator drive winch and part of the energy loss in the balance and multiple directional control valves.

## 4 Winch system modeling and simulation model

### 4.1 Winch system modeling

After the load weight  $F$  and the desired lifting and lowering speed  $v$  have been determined, the output power of the electric motor/generator-variable displacement hydraulic pump/motor is determined using Eq. 1.

$$P = \frac{F \cdot v}{1000} = \frac{2\pi n \cdot T}{6000} \quad (1)$$

where  $P$ ,  $n$ , and  $T$  are the output power, speed, and output torque of the electric/generator-variable hydraulic pump/motor, respectively.

The output power  $P$  includes two components: output torque  $T$  and output speed  $n$ . For the electric motor/generator-variable-displacement hydraulic pump/motor, the required output torque  $T$  is determined by the load weight  $F$ , the diameter of winch reducer  $D$ , and the winch reducer transmission ratio  $r$ , as shown in Eq. 2.

$$T = \frac{30F \cdot v}{\pi \cdot n} = \frac{F \cdot D}{2r} \quad (2)$$

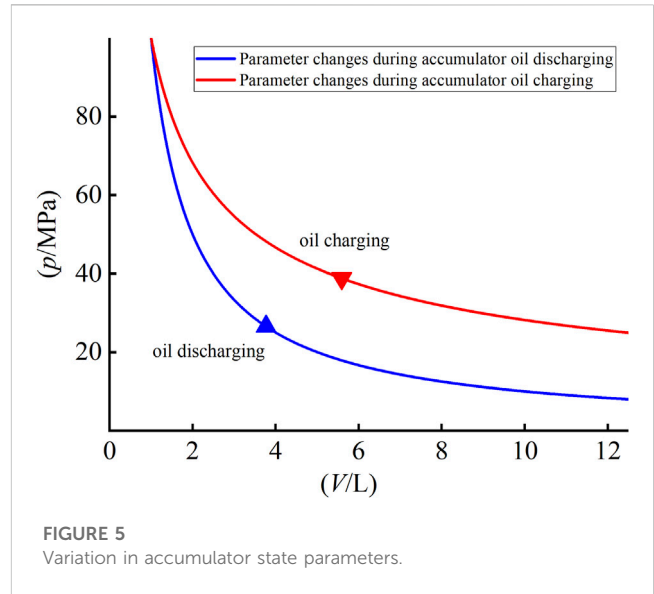
In the case of the electric motor/generator-variable-displacement hydraulic pump/motor, the desired velocity  $n$  can be determined by the desired lift and lowering velocity  $v$  of the weight, the diameter of the winch reducer  $D$ , and the winch reducer transmission ratio  $r$ , as shown in Eq. 3.

$$n = \frac{60v \cdot r}{\pi D} \quad (3)$$

The variable-displacement hydraulic pump/motor is designed to deliver a constant proportional torque. The displacement  $V$  of the variable displacement hydraulic pump/motor can be determined by  $\Delta p$ , as shown in Eq. 4

$$V = \frac{2\pi T}{\Delta p \cdot k} \quad (4)$$

where  $V$  is the displacement of the variable displacement hydraulic pump/motor, and  $k$  is the displacement influencing factor, the value of which is directly related to the output power assumed by the artificially desired variable displacement hydraulic pump/motor.  $T/k$  denotes the amount of output torque that must be assumed by the variable-displacement hydraulic pump/motor.



After the electric motor/generator speed has been controlled at the desired value and the displacement of the variable-displacement hydraulic pump/motor has been calculated, the required flow rate of the high-pressure accumulator  $q_1$  and low-pressure accumulator  $q_2$  can be calculated by Eq. 5.

$$q = n \cdot V \quad (5)$$

where  $q$  is the high-pressure and low-pressure accumulator flow rate.

The maximum pressures of the high-pressure and low-pressure accumulators are limited by the setting pressures of the first and second direct-acting relief valves, respectively. The setting pressures of the third and fourth direct-acting relief valves are determined by the system operating pressure. The first check valve, the second check valve, the first charge check valve, and the second charge check valve are not set to an initial pressure. Each 2-position 2-way electromagnetic valve has a fully open and a fully closed state. In the fully open state, the flow rate restriction or pressure drop at the inlet and outlet of the valve is as small as possible. Therefore, the differential pressure between the high-pressure and low-pressure accumulators can be approximated as that of the two ends of the variable displacement hydraulic pump/motor. The hydraulic system may not be capable of delivering constant proportional power due to the capacity limitations of the high-pressure and low-pressure accumulators. Thus, movement of the weight requires the electric motor/generator alone.

### 4.2 Winch system simulation model

According to the scheme presented in Figure 1 and the control strategy illustrated in Figure 3, the simulation model of the electro-hydraulic composite drive winch system is shown in Figure 4. The main components of the simulation model are the hydraulic system model, the signal control system model, and the mechanical system model.

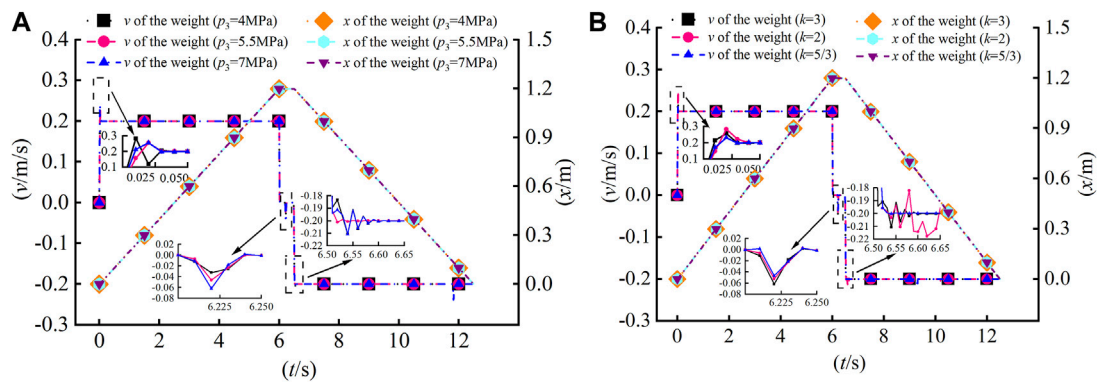


**FIGURE 6** Dynamic characteristics of the system under different conditions. (A) Different  $p_3$ . (B) Different  $k$ .

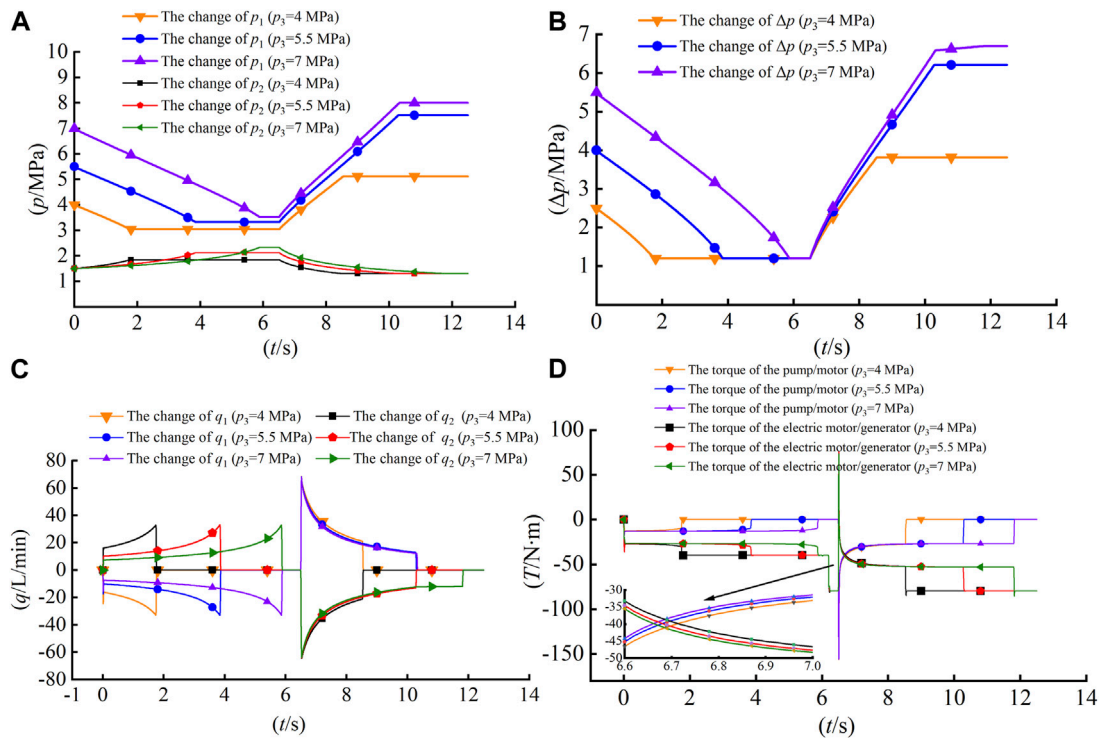


**FIGURE 7** Pressure and flow rate characteristic of the system at different  $p_3$ . (A) High-pressure and low-pressure accumulator pressure variation. (B) Differential pressure variation of the high-pressure and low-pressure accumulators. (C) Flow rates of the high-pressure and low-pressure accumulators. (D) Variation in the output torque of the electric motor/generator-variable hydraulic pump/motor.

The heavy-load mass, the light-load mass, the winch reduction ratio  $r$ , the reel diameter, and the maximum lifting and lowering velocity of the weight are defined as 3 t, 1 t, 55.2, 0.44 m, and 1.5 m/s respectively.

Calculated using Eq. 1, the maximum output powers required by the electric motor/generator-variable-displacement hydraulic pump/motor for heavy and light loads are 45 kW and 15 kW, respectively.

Calculated using Eq. 2, the maximum output torques required by the electric motor/generator-variable-displacement hydraulic pump/motor for the heavy and light loads are 120 N·m and 40 N·m, respectively.

Calculated using Eq. 3, the maximum weight-lowering speed required by the electric motor/generator-variable-displacement hydraulic pump/motor is 3,594 r/min.

The  $\Delta p_{\min}$  is controlled at around 1.2 MPa. The minimum  $k$  is set at 5/3, which means that 3/5 of the torque required by the system must be carried by the variable-displacement hydraulic pump/motor. The maximum  $V$  required by the variable-displacement hydraulic pump/motor for the heavy and light loads can be calculated using Eq. 4 as 450 mL/r and 150 mL/r, respectively.



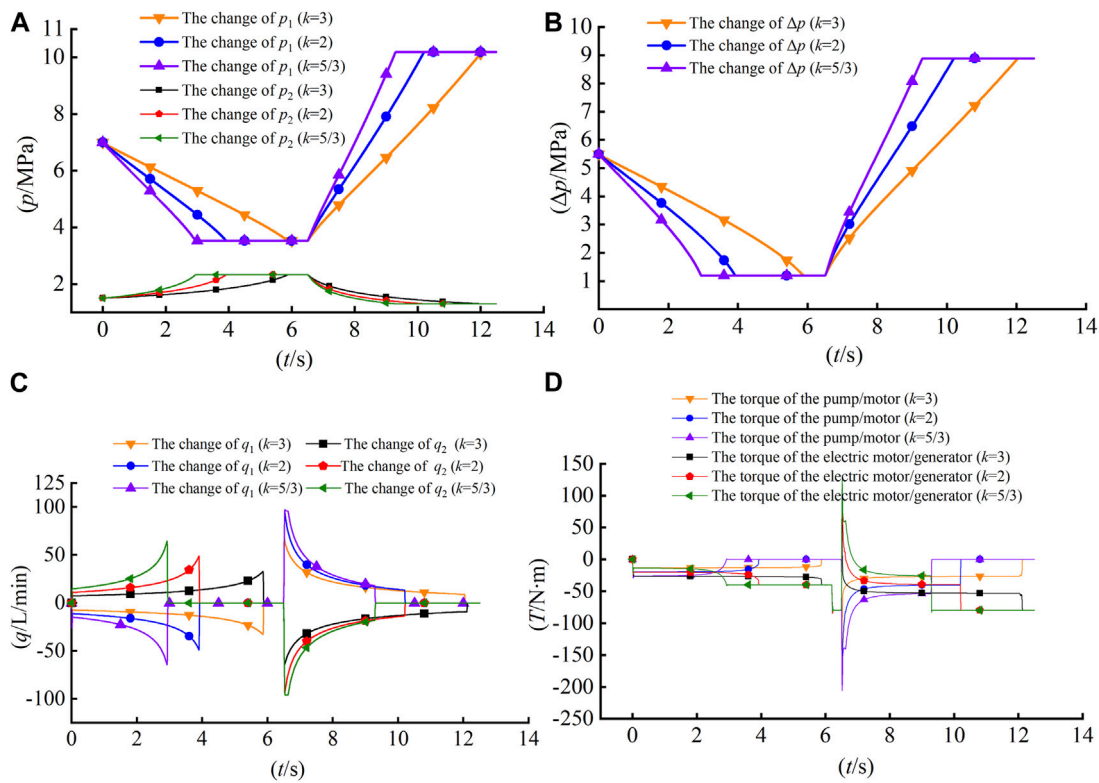


**FIGURE 8** Pressure and flow rate characteristics of the system at different  $k$  values. (A) High-pressure and low-pressure accumulator pressure variation. (B) Differential pressure variation for high-pressure and low-pressure accumulators. (C) Flow rate for high-pressure and low-pressure accumulators. (D) Variation of the output torque of the electric motor/generator-variable-hydraulic pump/motor.

Therefore, the variable-displacement hydraulic pump/motor with a maximum  $V$  of 500 mL/r is used in the system.

The rated power, the rated torque, and the rated speed of the electric motor/generator should be greater than the values calculated above. The initial state of charge of the lithium battery is set to 90%, and the capacity of the lithium battery is set to 6.5 Ah.

The main technical parameters required for the simulation of the electro-hydraulic composite drive winch system are shown in Table 1.

### 5 System simulation analysis

The simulation analysis focuses on the dynamic characteristics of the lifting cycle of the weight at different variable-displacement hydraulic pump/motor output proportional torques and initial pressures of the high-pressure accumulator, as well as the energy recovery efficiency of the system during the lowering of the weight.

#### 5.1 Dynamic characteristics of the weight under different conditions

The cycle time in the simulation is set to 12.5 s, where 0–6 s is the lifting condition, 6 s–6.5 s is the stop condition, and 6.5 s–12.5 s is the lowering condition. The expected lifting and lowering velocity is

0.2 m/s. The speed of the electric motor/generator-variable-displacement hydraulic pump/motor is controlled by the PID at 480 r/min. The dynamic characteristics of the weight lifting and lowering are studied under a different initial pressure of the high-pressure accumulator and output torque of the variable-displacement hydraulic pump/motor, respectively. As the  $\Delta p$  can be approximated as  $p_{BA}$ , it is set to  $\Delta p_{\min}$  (1.2 MPa) when the weight is lifting ( $F = 1t$ ) and to  $p_{2\min}$  (1.3 MPa) when the weight is lowering ( $F = 2t$ ). If the movement is not completed, the variable-displacement hydraulic pump/motor is put into an idle state by the VCU and no more power is outputted, while the remaining power is outputted by the electric motor/generator alone. During the simulation, SOC and  $F$  are set to  $F \geq F_{\min}$  and  $SOC \geq SOC_{\min}$ , and the system in the electro-hydraulic composite drive and energy recovery mode.

Owing to the advantages of good oil and gas isolation, high specific volume, and tightness, airbag accumulators are used for both high-pressure and low-pressure accumulators in the system. The high-pressure accumulator is set to 5 L with a pre-charge pressure of 2 MPa, while the low-pressure accumulator is set to 10 L with a pre-charge pressure of 0.5 MPa. The relationship between the volume  $V_1$  of the accumulator gas chamber and pressure is shown in Eq. 6.

$$pV_1^m = W \tag{6}$$

where  $W$  is constant and  $m$  is the state index varying between 1 and 1.4.

The trend of the accumulator state parameters during the charging and discharging of the accumulator can be obtained from Figure 5. Where the charging and discharging process curves do not coincide, the general expansion process of the gas (discharging process) is faster than the compression process (charging process).

### 5.1.1 Different initial pressures of the high-pressure accumulator

The purpose of this study was to investigate the dynamic characteristics of weight lifting and lowering under different initial high-pressure accumulator pressures from  $p_3$  to 4 MPa, 5.5 MPa, and 7 MPa. The initial pressure  $p_2$  is the same 1.5 MPa under different conditions. Moreover, the lift condition is such that  $k = 3$ , i.e., 1/3 of the total torque at a constant output of the variable-displacement hydraulic pump/motor. As shown in Figure 6A, the weight can quickly and more stably reach the target velocity loaded from a stop condition ( $t = 6.2$  s) and suddenly started from a stop condition to a lowering condition ( $t = 6.5$  s) with different  $p_3$ . This indicates that the proposed winch system has good dynamic characteristics.

When the weight is in the lifting condition (0–6 s), the lower the  $p_3$ , the smaller the initial  $\Delta p$  and  $p_{BA}$  ends of the variable-displacement hydraulic pump/motor. In cases with the same required torque and speed, according to Eq. 4; Eq. 5, the larger the initial  $V$  required, the larger the initial  $q_1$ . Accordingly, a larger  $q$  will flow into the low-pressure accumulator with the same initial  $p_2$  (1.5 MPa). For the system with lower  $p_3$ , as shown in Figures 5, 7A and Eq. 6 show that  $p_2$  rises faster. The faster that  $p_{BA}$  falls, the faster that  $V$  will rise. As shown in Figure 7C, the  $q_1$  will rise faster, the flow rate into the corresponding high-pressure and low-pressure accumulators will also rise, and the pressure will rise faster. As shown in Figures 7B, D, the faster the differential pressure reaches  $\Delta p_{min}$  (1.2 MPa), the faster the variable-displacement hydraulic pump/motor will be in an idle state without output torque, and the motor/generator will output torque separately during the lifting condition.

When the weight is in the stop condition (6 s–6.5 s), the load weight is lifted from 1 t to 2 t at 6.2 s and changed from the stop condition to the lower condition at 6.5 s. As shown in Figures 6A, 7B, D and Eq. 10, no sliding down of twice the weight occurs owing to the instantaneous high torque provided by the electric motor/generator and variable-displacement hydraulic pump/motor. The  $\Delta p$  is always 1.2 MPa during this period.

When the weight is in the lowering condition (6.5 s–12.5 s), for the system with a different  $p_3$ , the  $\Delta p$  is initially the same at 1.2 MPa. When the required torque and speed are the same, according to Eq. 4; Eq. 5, the required  $V$  and  $q_2$  are also the same. For the system with higher  $p_3$ , as shown in Figure 7B shows that in the lowering condition, the faster that the  $\Delta p$  rises, the faster the pressure difference between the two ends of the variable-displacement hydraulic pump/motor rises, and the faster that  $V$  will fall. As shown in Figure 7C,  $q_2$  will fall faster. It is reasonable to say that in the system with a higher  $p_3$ , the slower that the pressure of the corresponding high-pressure accumulator will rise and the slower that the pressure of the low-pressure accumulator will fall during the lowering process. For the system with a higher  $p_3$ , the initial  $p_1$  and  $p_2$  are higher. Combined with Figure 5; Figure 7B; Eq. 6 show that in

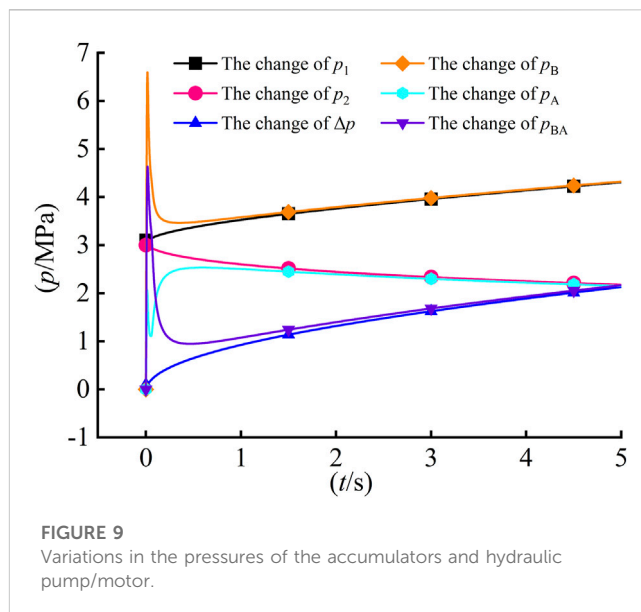


FIGURE 9 Variations in the pressures of the accumulators and hydraulic pump/motor.

the system with the higher  $p_3$ , the faster the  $\Delta p$  and the pressure difference between the two ends of the variable-displacement hydraulic pump/motor will rise during the entire lowering process. As shown in Figures 7A,D, the faster the  $p_2$  reaches  $p_{2min}$  (1.3 MPa), the faster the variable-displacement hydraulic pump/motor will be in an idle state without output torque, and the motor/generator will output torque separately during the lowering condition.

### 5.1.2 Different variable-displacement hydraulic pump/motor output proportional torque

For  $k = 3$ ,  $k = 2$ , and  $k = 5/3$ , we expect 1/3, 1/2, and 3/5 of the total torque at a constant output of the variable-displacement hydraulic pump/motor and observe the dynamic characteristics of the lifting and lowering of the mass. When  $p_3$  is 7 MPa, the initial  $p_2$  is 1.5 MPa. As shown in Figure 6B, the dynamic characteristics of this winch system are all good for different  $k$  values. The weight can quickly and more stably reach the target velocity when loaded from a stop condition ( $t = 6.2$  s) and when suddenly starting from a stop condition to a down condition ( $t = 6.5$  s).

When the weight is in the lifting condition (0–6 s), the initial pressures of the high-pressure and low-pressure accumulators are the same for systems with different  $k$  values. The initial  $\Delta p$  is the same. The initial differential pressure between the two ends of the variable-displacement hydraulic pump/motor is the same. For the system with larger proportional torque output, in the case of the same required speed according to Eq. 4, the larger the required initial  $V$ , the larger the initial  $q_1$ . According to Eq. 5 and as shown in Figure 5 and Eq. 6, the faster the  $p_1$  falls and  $p_2$  rises, the faster the pressure difference between the two ends of the variable-displacement hydraulic pump/motor falls and the faster the  $V$  will rise. As shown in Figure 8C, the  $q_1$  will rise faster. The corresponding  $q_2$  and  $p_2$  will also rise faster. As shown in Figures 8B, D, the faster the differential pressure reaches  $\Delta p_{min}$  (1.2 MPa), the faster the variable displacement hydraulic pump/motor will be in

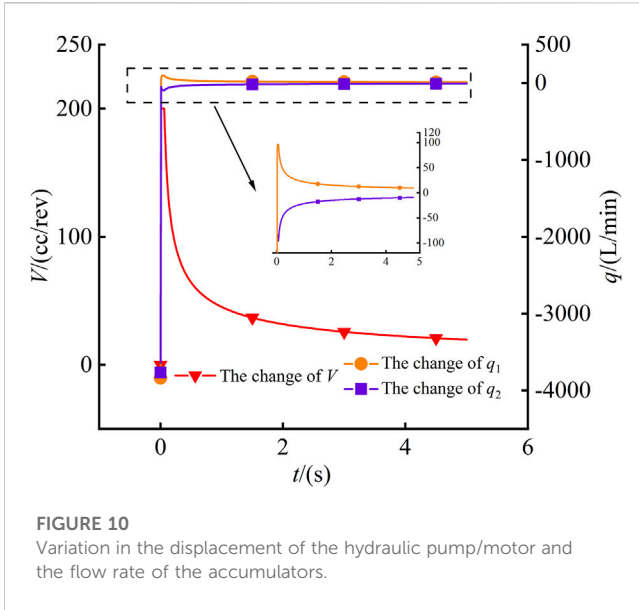


**FIGURE 10**  
Variation in the displacement of the hydraulic pump/motor and the flow rate of the accumulators.

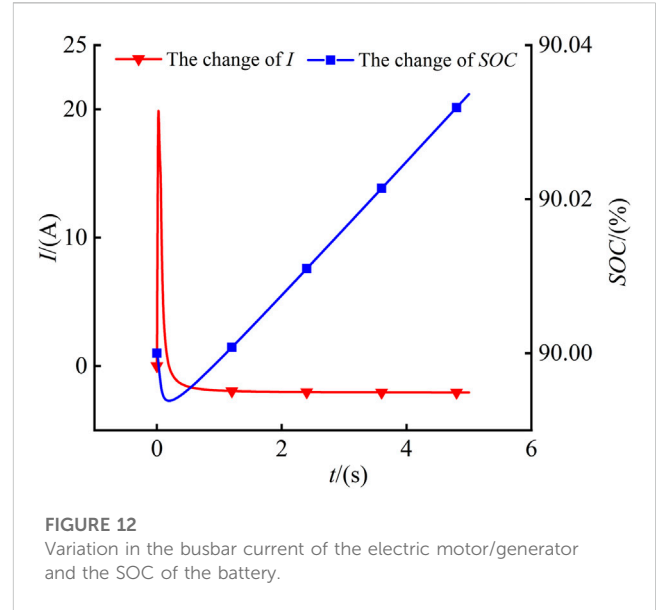


**FIGURE 12**  
Variation in the busbar current of the electric motor/generator and the SOC of the battery.

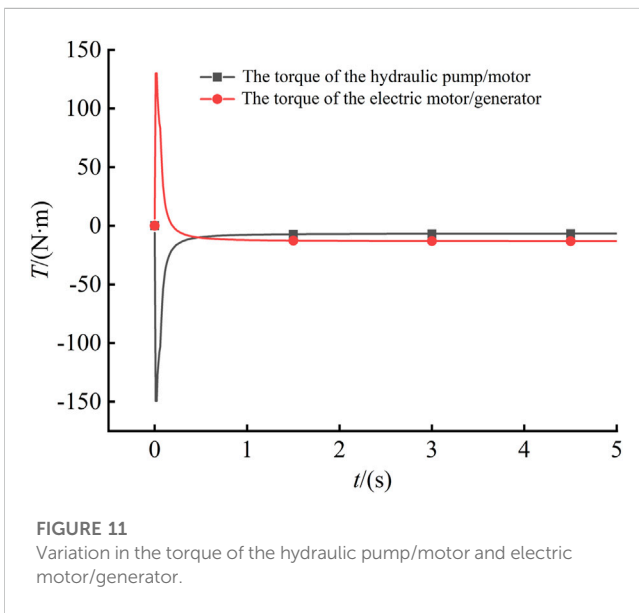


**FIGURE 11**  
Variation in the torque of the hydraulic pump/motor and electric motor/generator.

an idle state without torque output and the motor/generator will separately output torque during the lifting condition.

When the weight is in the stop condition (6 s–6.5 s), the load weight is lifted from 1 t to 2 t at 6.2 s and changed from the stop condition to the lower condition at 6.5 s. As shown in Figures 6B, Figures 8B,D and Eq. 10, no sliding down of twice the weight occurs owing to the instantaneous high torque provided by the electric motor/generator and variable-displacement hydraulic pump/motor. The  $\Delta p$  is always 1.2 MPa during this period.

When the weight is in the lowering condition (6.5 s–12.5 s), for the different  $k$  in the system, the initial  $\Delta p$  is always 1.2 MPa. For the system with larger  $k$ , in the case of the same required speed according to Eq. 4; Eq. 5 shows that the required initial  $V$  and initial  $q_2$  are larger. Figure 5 and Eq. 6 show that the faster the  $p_2$  falls and the  $p_1$  rises, the faster  $p_{BA}$  rises, and the faster the  $V$  will fall. As

shown in Figure 8C, the  $q_2$  will fall faster; thus, it is reasonable to say that the higher the  $k$ , the slower the corresponding  $p_1$  will rise and the corresponding  $p_2$  will fall during the lowering process. The system with the higher proportional torque output of the variable-displacement hydraulic pump/motor during the whole lower process can still rely on its higher torque required to maintain the  $q$  at a higher level even when the  $q$  falls, as shown in Figure 8C. The combination of Figures 5, 8A, B, and Eq. 6 shows that the higher the proportional torque of the variable-displacement hydraulic pump/motor outputs during the whole lower process, the faster  $p_1$  rises, the faster  $p_2$  falls, and the faster  $\Delta p$  rises. As shown in Figures 8B, D, the faster that  $p_2$  reaches  $p_{2min}$  (1.3 MPa), the faster the variable-displacement hydraulic pump/motor will be in an idle state without output torque, and the motor/generator will output torque separately during the lowering condition.

## 5.2 Analysis of the efficiency of the system energy recovery

The energy recovery efficiency of the winch system is discussed in terms of the power of the high-pressure accumulator, the power of the low-pressure accumulator, the power of the electric motor/generator, and the power consumption of the lowering weight. The energy can be obtained by integrating the corresponding power of each component. The system is in the recovery mode of the electro-hydraulic composite drive during the descent, i.e.,  $p_2 \geq p_{2min}$ . The  $\Delta p$  in the simulation process can be treated as  $p_{BA}$ . The whole simulation system is first in the electro-hydraulic composite drive and energy recovery mode. The battery SOC and the load weight  $F$  are treated as  $F \geq F_{min}$  and  $SOC \leq S_{max}$ , respectively.

The power of the high-pressure accumulator  $P_1$  and the low-pressure accumulator  $P_2$  are determined using Eq. 7 and Eq. 8.

$$P_1 = p_1 \cdot q \tag{7}$$

$$P_2 = p_2 \cdot q \tag{8}$$

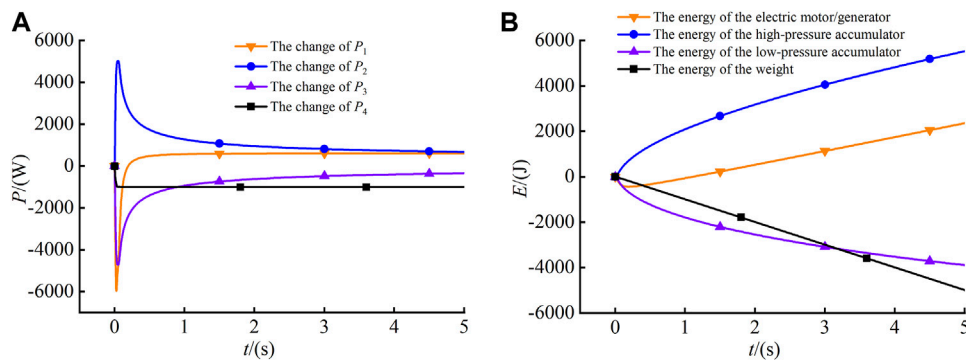


**FIGURE 13** Variation in the power and energy of each component. (A) Variation in the power of each component. (B) Variation in the energy of each component.

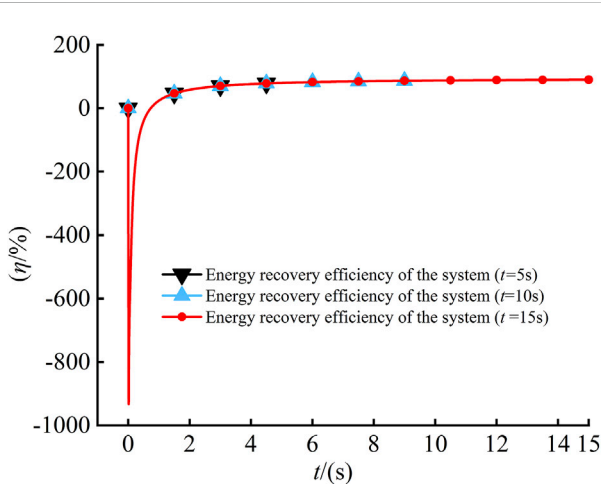


**FIGURE 14** Energy recovery efficiency at different distances of weight descent.

The power of the electric motor/generator  $P_3$  can be calculated from Eq. 9.

$$P_3 = U \cdot I \tag{9}$$

where  $U$  and  $I$  represent the busbar voltage and current of the electric motor/generator, respectively. The electric motor/generator is in the electric motor state when  $I > 0$  and in the electric generator state when  $I < 0$ .

The power of the lowering weight  $P_4$  can be determined by the weight lowering height  $s$  and  $F$ , as shown in Eq. 10.

$$P_4 = F \cdot s \tag{10}$$

The energy recovery efficiency of the system  $P_5$  is determined using Eq. 11.

$$P_5 = \frac{P_1 - P_2 + P_3}{P_4} \cdot 100\% \tag{11}$$

After setting  $F = 0.5t$ ,  $k = 3$ , and  $v = 0.2\text{m/s}$ , the energy recovery efficiency of the system is investigated for a weight-

lowering height of 1 m ( $s = 1\text{m}$ ). All the 2-position 2-way electromagnetic valves are controlled in the de-energized state before lowering the weight. As shown in Figure 9, no pressure is built up at the two ends of the variable-displacement hydraulic pump/motor, i.e.,  $p_{BA} = 0$  at  $t = 0\text{s}$ . Combined with Figure 10 and Eq. 4, these results show that the variable-displacement hydraulic pump/motor must adapt itself to rapidly increase  $V$  to deliver a certain torque when the weight suddenly starts to lower. As shown in Figure 10 and Eq. 5, the higher the  $V$ , the higher the  $q$ . As shown in Figure 13A,  $P_1$  and  $P_2$  both are large at the initial moment according to Eq. 7 and Eq. 8. The higher the  $q_1$  and  $q_2$ , the greater the changes in the gas volumes of the high-pressure and low-pressure accumulators. As shown in Figure 5 and Eq. 6, the greater the changes in the gas volume of the high-pressure and low-pressure accumulators, the higher the changes in  $p_1$  and  $p_2$ . As shown in Figure 9,  $p_1$ ,  $\Delta p$ , and  $p_{BA}$  rise, while  $p_2$  falls quickly after the weight has been lowered. As shown in Figure 10,  $V$  cannot be reduced in time due to the delay in system control after a rapid increase in  $p_{BA}$ . According to Eq. 4 and as shown in Figure 11, the variable-displacement hydraulic pump/motor output torque momentarily exceeds its required output by 1/3 proportional torque in the hydraulic pump state. At the same time, as shown in Figure 11, Figure 12, and Eq. 9, the positive torque output of the electric motor/generator ensures that the system outputs a constant torque; the busbar current  $I$  is  $> 0$  meaning that the electric motor/generator is in the electric motor state; i.e., the SOC of the battery is consumed. Combined with Figure 13A, Figure 13B, Figure 14, and Eq. 11, the electric motor/generator is in the electric motor state, which means that  $P_3 < 0$  is the main reason why  $P_5 < 0$  at the initial moment. As shown in Figure 10, Figure 11, and Figure 12, the variable-displacement hydraulic pump/motor and the electric motor/generator can output a constant proportional torque respectively;  $I < 0$  and  $P_3 > 0$  means the electric motor/generator is in the electric generator state; i.e., the SOC of the battery is stored after  $V$  has returned to its normal range of variation. As shown in Figure 9, Figure 10, Figure 13A, Eq. 7, and Eq. 8, as  $p_1$  increases, so does  $P_1$ ; similarly, as  $p_2$  increases, so does  $P_2$ . As shown in Figure 14 and Eq. 11, the longer the weight is lowered, the greater the  $P_5$ .

## 6 Conclusion

To recover the gravitational potential energy and avoid secondary sliding, this study proposed an electro-hydraulic composite drive winch and energy recovery system for mobile cranes. The problems of secondary sliding of the weight and the limited energy recovery of the accumulator can be solved effectively by the high energy density of the lithium batteries and the good control characteristics of the electric motor/generator. The problem of high energy consumption of the electric motor/generator drive winch and most of the energy consumption of the liquid drive winch in the balance and multiple directional control valves can be alleviated by instantaneous high-power density and large torque output at the near-zero speed of the accumulator-variable displacement hydraulic pump/motor.

The feasibility of the control strategy of the electro-hydraulic composite drive winch and potential energy recovery system was verified through the study of the dynamic characteristics of the weight lifting and lowering under different conditions. We studied the pressure variations of the high-pressure and low-pressure accumulators ( $p_1$  and  $p_2$ ), as well as the pressure difference ( $\Delta p$ ), flow rate ( $q$ ), and output torque of the electric motor/generator-variable displacement hydraulic pump/motor ( $T$ ). When  $p_3$  or  $k$  is at different values in this electro-hydraulic composite drive winch system, the weight lifting and lowering dynamic characteristics differ.

The energy recovery efficiency of the electro-hydraulic composite drive winch and potential energy recovery system control strategy was higher for weights lowered a greater distance. Although the energy recovery efficiency of the system was high in the final results, the magnitude of the final recovery efficiency could be influenced by changing the initial pressure and volume of the high-pressure and low-pressure accumulators as well as the fixed voltage of the lithium battery. The specific energy recovery efficiency is for reference only and must be considered in conjunction with the actual situation. The system control strategy is mainly based on the detection of load weight  $F$ , battery SOC, high-pressure and low-pressure accumulator pressure, etc., to determine the drive mode of the weight. The electro-hydraulic composite drive mode can reasonably use the motor speed active control to achieve variable-displacement hydraulic pump/motor adaptive speed. Automatic adjustment of the displacement of the variable-displacement hydraulic pump/motor is used to actively control the torque and, thus, achieve adaptive torque compensation of the electric motor/generator.

The energy recovery efficiency of the system in this study may vary considerably under different initial conditions. The basis for the high efficiency of the energy recovery of the system is the selection of suitable initial conditions in the actual working process. The efficiency of the energy recovery is not considered in this system when the initial pressure ( $p_1$  and  $p_2$ ) and volume of the high-pressure and low-pressure accumulators and the performance parameters of the lithium battery are changed. The results of this study lay a foundation for further experimental research.

## References

Bolonne, S. R. A., and Chandima, D. P. (2019). Sizing an energy system for hybrid Li-ion battery-supercapacitor RTG cranes based on state machine energy controller. *Ieee Access* 7, 71209–71220. doi:10.1109/access.2019.2919345

## 7 Research ethics

The study does not involve animal or human subjects and does not contain identifiable human data.

## Data availability statement

The raw data supporting the conclusion of this article will be made available by the authors, without undue reservation.

## Author contributions

XX and TL contributed to the direction of the research content, study design, manuscript writing, data processing, and data analysis. HR and TG contributed to the literature searches and data collection. ZL and CM were mainly responsible for data analysis and project management. All authors contributed to the article and approved the submitted version.

## Funding

This work was supported by the National Key Research and Development Program (2020YFB2009900), the National Natural Science Foundation of China (Grant No. 52275055), Key Projects of the Natural Science Foundation (Grant No. 2021J02013).

## Acknowledgments

We thank all the authors for completing the study and acknowledge the valuable comments and constructive suggestions of the editor and reviewers.

## Conflict of interest

The authors declare that the research was conducted in the absence of any commercial or financial relationships that could be construed as a potential conflict of interest.

## Publisher's note

All claims expressed in this article are solely those of the authors and do not necessarily represent those of their affiliated organizations, or those of the publisher, the editors, and the reviewers. Any product that may be evaluated in this article, or claim that may be made by its manufacturer, is not guaranteed or endorsed by the publisher.

Caporali, R. P. L. (2021). Anti-sway method for reducing vibrations on a tower crane structure. *Int. J. Nonlinear Sci. Numer. Simul.* 24, 171–184. doi:10.1515/ijnsns-2021-0046



- Corral-Vega, P. J., Garcia-Trivino, P., and Fernandez-Ramirez, L. M. (2019). Design, modelling, control and techno-economic evaluation of a fuel cell/supercapacitors powered container crane. *Energy* 186, 115863. doi:10.1016/j.energy.2019.115863
- Fang, X., Zhao, H., and Liu, P. (2012). Simulation study of main winch system geopotential energy recovery in rotary driller. *Eng. J. Wuhan Univ.* 45, 241–245+272.
- Huang Pu, H. (2015). *Study of ultracapacitor-based power compensation and energy Recovery system for mine lifting equipment*. Beijing: Beijing Jiaotong University.
- Kim, K., An, J., Park, K., Roh, G., and Chun, K. (2019). Analysis of a supercapacitor/battery hybrid power system for a bulk carrier. *Appl. Sciences-Basel* 9. doi:10.3390/app9081547
- Kodkin, V. L., and Anikin, A. S., (2020) The reflection mode of the moment loads by an asynchronous electric drive with vector control and the features of this mode in the rotation drive of the tower crane", in: International Ural Conference on Electrical Power Engineering, 22-24 September 2020, Russia.
- Lee, J.-G., Yeo, H.-K., Jung, H.-K., Kim, T.-K., and Ro, J.-S. (2019). Electromagnetic and thermal analysis and design of a novel-structured surface-mounted permanent magnet motor with high-power-density. *Iet Electr. Power Appl.* 13, 472–478. doi:10.1049/iet-epa.2018.5322
- Li, K., and Wang, Y. (2019). Maximum torque per ampere (MTPA) control for IPMSM drives using signal injection and an MTPA control law. *Ieee Trans. Industrial Inf.* 15, 5588–5598. doi:10.1109/tii.2019.2905929
- Li, X., Cao, S., Luo, M., and Sun, L. (2022). Design and control strategy of energy recovery device for pure electric vehicle crane. *Constr. Mach. Equip.* 53, 104–108+113.
- Lin, T., Lin, Y., Ren, H., Chen, H., Chen, Q., and Li, Z. (2020). Development and key technologies of pure electric construction machinery. *Renew. Sustain. Energy Rev.* 132, 110080. doi:10.1016/j.rser.2020.110080
- Liu, H., Quan, L., Hao, Y., Huang, J., Li, Y., and Liu, Y. (2022). Fabrication of superhydrophobic coating based on waterborne silicone-modified polyurethane dispersion and silica nanoparticles. *Chin. Hydraulics Pneumatics* 46, 22–29. doi:10.3390/polym15010022
- Liu, J. (2019). China's renewable energy law and policy: A critical review. *Renew. Sustain. Energy Rev.* 99, 212–219. doi:10.1016/j.rser.2018.10.007
- Premkumar, K., and Manikandan, B. V. (2014). Adaptive neuro-fuzzy inference System based speed controller for brushless DC motor. *Neurocomputing* 138, 260–270. doi:10.1016/j.neucom.2014.01.038
- Roman, R.-C., Precup, R.-E., and Petriu, E. M. (2021). Hybrid data-driven fuzzy active disturbance rejection control for tower crane systems. *Eur. J. Control* 58, 373–387. doi:10.1016/j.ejcon.2020.08.001
- Wang, X., Ge, L., Zhao, B., Hao, Y., Quan, L., and Mu, X. (2020). Energy efficiency characteristics of cable shovel lifting system driven by hydraulic-electric hybrid system. *Trans. Chin. Soc. Agric. Mach.* 51, 418–426. [In Chinese].
- Zhang, H. (2019). *Research on energy saving technology of hydraulic truck crane*. Dalian: Dalian Ligong University. [master's thesis].
- Zhang, J., Zhao, B., Hao, Y., Yu, H., Wang, J., Lei, A., et al. (2020). Pluripotent stem cell-derived CAR-macrophage cells with antigen-dependent anti-cancer cell functions. *Chin. Hydraulics&Pneumatics* 13, 153–160. [In Chinese]. doi:10.1186/s13045-020-00983-2
- Zhang, Y.-J., Peng, Y.-L., Ma, C.-Q., and Shen, B. (2017). Can environmental innovation facilitate carbon emissions reduction? Evidence from China. *Energy Policy* 100, 18–28. doi:10.1016/j.enpol.2016.10.005
- Zhao, B., Quan, L., and Hao, Y. (2016). Research of operating characteristics and energy efficiency of traction elevator with hybrid electric-hydraulic drive. *J. Mech. Eng.* 52, 192–198. doi:10.3901/jme.2016.04.192
- Zhu, J., Wang, P., Wu, H., and Zhu, Z. (2018). Guan (Care/Control): An ethnographic understanding of care for people with severe mental illness from shanghai's urban communities. *Mach. Des. Manuf.* 42, 92–111. doi:10.1007/s11013-017-9543-x